Signature for Vibrational to Rotational Evolution Along the Yrast Line

P. H. Regan,[1,2] C. W. Beausang,[1] N. V. Zamfir,[1,3,4] R. F. Casten,[1] Jing-ye Zhang,[1,5] A. D. Yamamoto,[1,2] M. A. Caprio,[1] G. Gürdal,[1,4] A. A. Hecht,[1] C. Hutter,[1] R. Krücken,[1] S. D. Langdown,[1,2] D. A. Meyer,[1] and J. J. Ressler[1]

[1]*Wright Nuclear Structure Laboratory, Yale University, New Haven, Connecticut 06520-8124*
[2]*Department of Physics, University of Surrey, Guildford GU2 7XH, United Kingdom*
[3]*Clark University, Worcester, Massachusetts, 01610*
[4]*National Institute for Physics and Nuclear Engineering, Bucharest-Magurele, Romania*
[5]*University of Tennessee, Knoxville, Tennessee 37996*

(Received 15 August 2002; published 18 April 2003)

We present a simple method for discerning the evolution from vibrational to rotational structure in nuclei as a function of spin. The prescription is applied to the yrast cascades in the $A \sim 110$ region and a clear transition from vibrational to rotational motion is found.

DOI: 10.1103/PhysRevLett.90.152502 PACS numbers: 21.10.Re, 21.60.Ev, 27.60.+j

Shape and phase evolution are major themes in nuclear structure research. This evolution is intimately related to the mechanisms by which atomic nuclei generate angular momentum. Although nuclei are composed of interacting fermions, examples of collective excitations resulting in both oscillations and rotations are well established. These collective modes manifest their angular momentum generation in different ways, resulting in contrasting excited state sequences and transition rates. For a theoretical, harmonic quantum vibrator, the yrast level energies for states of spin I are given by $E_I = n\hbar\omega$ [1], where the phonon number $n = \frac{I}{2}$ and the reduced matrix element between yrast states differing by $\Delta I = 2$ is proportional to $\sqrt{n}$. For a perfect axially symmetric rotor, the energy sequence is given by $E_I = [\hbar^2/(2J)]I(I+1)$ [2], where J is the static moment of inertia and the $B(E2)$ values tend to a constant value at high spins.

Rotational interpretations such as the cranked shell model (CSM) [3] are mainstream tools in the analysis of yrast states. The application of this model has been spectacularly successful in interpreting much experimental data, particularly with respect to understanding the microscopical basis behind the phenomenon of "backbending" [3], which has been explained for rotational, deformed nuclei as stemming from a Coriolis-driven particle alignment [4]. In a standard CSM-type analysis, in order to compare the model predictions with experimental data, a rotational approximation is applied (usually based on the variable moment of inertia prescription) and an effective, spin dependent moment of inertia extracted.

The purpose of this Letter is to point out that, while such a prescription remains valid for well deformed systems, its use for nonrotational (e.g., vibrational) nuclei may obscure interesting structural effects, such as the transition between vibrational and rotational collective modes as a function of nuclear spin. We will propose a new approach, called E-GOS (E-Gamma Over Spin) curves, which invokes no structural preconceptions and allows vibrational and rotational behavior, and the transition between the two, to be vividly highlighted.

The gamma-ray decay energies for a perfect harmonic vibrator are given by $E_\gamma(I \to I-2) = \hbar\omega$ while, for an axially symmetric rotor, $E_\gamma(I \to I-2) = [\hbar^2/(2J)] \times (4I-2)$. The ratio, $R = \frac{E_\gamma(I \to I-2)}{I}$ then provides an effective way of distinguishing axially symmetric rotational and harmonic vibrational modes.

$$\text{vibrator}: \qquad R = \frac{\hbar\omega}{I} \xrightarrow{I\to\infty} 0, \tag{1}$$

$$\text{rotor}: \qquad R = \frac{\hbar^2}{2J}\left(4 - \frac{2}{I}\right) \xrightarrow{I\to\infty} 4\left(\frac{\hbar^2}{2J}\right). \tag{2}$$

For the idealized axially symmetric rotor, R increases from $3[\hbar^2/(2J)]$, for $I = 2$, to a constant value of $4[\hbar^2/(2J)]$ for large I while, for a pure vibrator, R decreases hyperbolically towards zero. (Note that, in the rotational model, R is equivalent to 2 divided by the kinematic moment of inertia but, since deformation is implicit in this concept, such definitions may be misleading for nonrotor nuclei.)

Figure 1(a) shows these theoretical limits plotted for two schematic nuclei: (i) a vibrator in which the first 2^+ excited state lies at an energy of 500 keV; and (ii) a rotor where this energy is 100 keV. (These values were taken to represent typical nuclear vibrator and rotor energies, respectively.) Note that the curvatures of the vibrator and rotor functions are markedly different. The sharp, hyperbolic decrease in R with spin provides a clear signature of a vibrational nucleus since, by contrast, for a rotor, R actually *increases* at low spins. We, thus, propose plots of $R = [E_\gamma(I \to I-2)/I]$ versus I as a simple prescription for distinguishing rotational and vibrational ranges of spin. We call the trajectories in such plots "E-GOS" curves. Note, R is an experimentally determined quantity based on well-defined observables, and includes no rotational ansatz nor the model-based concepts of rotational frequency and moment of inertia.

As an example of the physics which can be extracted and also to highlight the inherent dangers of simply

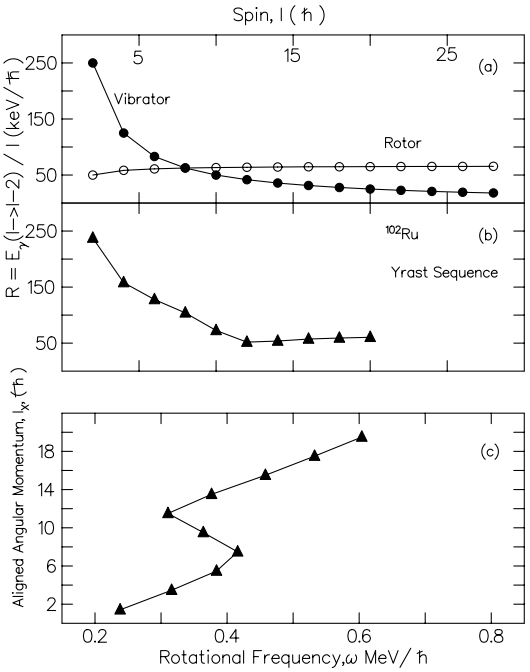

FIG. 1. (a) E-GOS curves for a perfect harmonic vibrator and axially symmetric rotor with first 2^+ excitations of 500 and 100 keV, respectively. (b) E-GOS plot for the yrast sequence in ^{102}Ru. (c) Total aligned angular momentum for the yrast sequence in ^{102}Ru as a function of rotational frequency.

assuming the rotational model over the entire spin range, Fig. 1(b) shows the empirical E-GOS curve for the yrast sequence of stretched E2 transitions in ^{102}Ru, while Fig. 1(c) highlights the same data on a standard quasiparticle alignment plot. Figure 2 shows the partial decay scheme for ^{102}Ru from which the data shown in Fig. 1 were taken. These data come from a recent experiment performed at the Wright Nuclear Structure Laboratory at Yale where the nucleus of interest was populated using the reaction ^{96}Zr(^{9}Be, $3n$)^{102}Ru at a beam energy of 44 MeV. The γ-ray transitions were detected using the YRASTBALL array [5] and the full experimental details

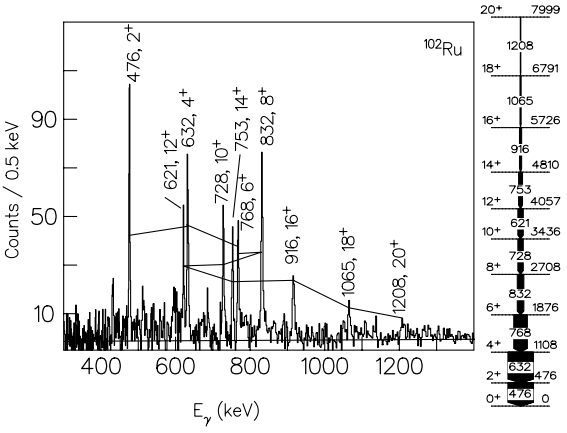

FIG. 2. Sum of triple gamma-ray gates showing the yrast sequence for ^{102}Ru in the current work.

can be found in Ref. [6]. The spectrum in Fig. 2 shows a sum of triple gates on the yrast sequence, which extends this structure from the ground state to the yrast spin $20\hbar$ level. The lower-spin yrast states of this nucleus confirm those in the literature [7].

As Fig. 1(c) shows, the standard rotational model analysis suggests a signature for rotationally driven alignment in this system. The backbending in Fig. 1(c), associated with an increase in total aligned angular momentum, $I_x = \sqrt{I(I+1)}$, of approximately $10\hbar$ is consistent with the neutron $h_{11/2}$ alignment predicted by CSM calculations [6]. In the framework of the CSM, this behavior would be interpreted as the standard change in the moment of inertia between two rotational phases following a Coriolis-driven pair breaking. However, as Fig. 1(b) clearly demonstrates, the E-GOS plot for the same data allows an alternative interpretation, namely, the evolution from a vibrational structure to a rotational sequence above spins of $(10–12)\hbar$. This interpretation does not require a rotational phase at lower spin, but rather implies a crossing between a deformed minimum and the (anharmonic) vibrational ground state configuration. Note that the ratio of excitation energies for the yrast 4^+ and 2^+ states in ^{102}Ru is 2.32, a value usually associated with an anharmonic vibrational system, which suggests the latter, nonrotational explanation.

The vibration-to-rotational transition can be explained microscopically by the population of a 10^+ state, with a wave function predominantly consisting of the maximally aligned coupling of two $h_{11/2}$ neutron orbitals [8]. Since these specific orbitals reside low in the $h_{11/2}$ subshell, they have large components of angular momentum along the rotation axis (i.e., small Ω values). They can, thus, be thought of as "polarizing" the potential to a shape with a small, but rigid quadrupole deformation, thus allowing collective rotational motion to develop. Note, it is the inducement of this small but rigid quadrupole deformation which has been proposed as the mechanism which allows "antimagnetic" rotational structures to evolve [9]. Such sequences have been reported in ^{100}Pd, built on top of the $I^\pi = 10^+$ aligned neutron configuration [10]. In these cases, the stiff, deformed potential formed by the population of this configuration allows weakly deformed rotational-like sequences to evolve following the gradual alignment of the proton $g_{9/2}$ angular momentum vectors along the now well-defined axis of rotation.

The data on ^{102}Ru shown in Fig. 1 demonstrate how both the standard "alignment" and the vibration-to-rotation pictures for this sequence can be obtained from a manipulation of the same data. We argue that this case highlights the potential dangers of applying a rotational-based approximation to low-spin states in "vibrational" nuclei where such concepts are not well defined. Although it is well known that one can plot a vibrational sequence on a backbending plot (i.e., the kinematic moment of inertia, $J^{(1)} = \frac{I}{\omega}$ versus rotational frequency, $\omega \approx \frac{E_\gamma}{2}$) as

a vertical line, this is somewhat physically misleading, since the quantity which is being plotted as a constant value, namely, the rotational frequency, has no definition outside the confines of a deformed, rotational paradigm. While a similar effect can also be demonstrated by plotting other variations of energy and spin variables, we propose that the major advantages of using the E-GOS prescription are that (i) it uses a linearly increasing variable on the x axis; (ii) it assumes no *a priori* (rotational) model interpretation; and (iii) it clearly and simply highlights the transition between vibrational and rotation states. In contrast, for example, a plot of excitation energy $E(I)$ against spin is qualitatively similar for both a vibrator and a rotor: Both trajectories are monotonically increasing functions with spin (albeit at quantitatively different rates), while in an E-GOS plot, one decreases sharply, whereas the other is a slightly increasing function and asymptotically flat.

The phenomena of a vibration-to-rotational crossing appears to be prevalent in many nuclei in this region, as we shall discuss below, in the context of E-GOS plots. The low-lying states in nuclei with $A \approx 110$ and $Z < 50$ have long been proposed as among the best examples of quadrupole vibrational structures in the nuclear chart [11]. Such nuclei are characterized by sequences of multiphonon excitations, which have been identified in the Cd ($Z = 48$ [12,13]), Pd ($Z = 46$ [14]), and Ru ($Z = 44$ [15]) isotopes, with up to five phonon (i.e., $n = 5$) states being observed [12]. Interestingly, where the data exist, the higher-spin yrast states of many of these nominally vibrational nuclei often demonstrate a weakly deformed behavior, with sequences of stretched E2 transitions which can be described as rotational bands (see, e.g., [16–23]). Although the predicted quadrupole deformations in these systems are generally rather small ($\beta_2 \sim 0.15$), these small deformations give rise to very large Coriolis effects [4], which in turn lead to the observation of what are described in the CSM as rotational alignments. Where published information exists (e.g., ^{108,110}Cd [24]), the E2 transition rates in the nominally vibrational and rotational parts of the decay schemes are similar ($20 \rightarrow 50$ Wu) and thus cannot be used to distinguish directly between vibrational and rotational-like excitations. As outlined above, the first yrast crossing in this region has been explained by numerous authors [7,16–23,25] as arising following the rotational alignment of a pair of low-Ω $h_{11/2}$ neutrons. However, we argue that, while the structure *above* the backbend may be clearly assigned as "rotational," the low-spin precursor structure is ambiguous in an alignment plot, but readily visible using the E-GOS prescription.

Figure 3 shows the E-GOS curves for the stretched E2 yrast sequences for the even-even nuclei between $Z = 42 \rightarrow 48$ and $N = 56 \rightarrow 66$. In some cases, there is a distinct evolution from the hyperbolic locus expected for vibrational structures to the near constant limit associated with rotational motion. Specifically, the $N = 58$ isotones

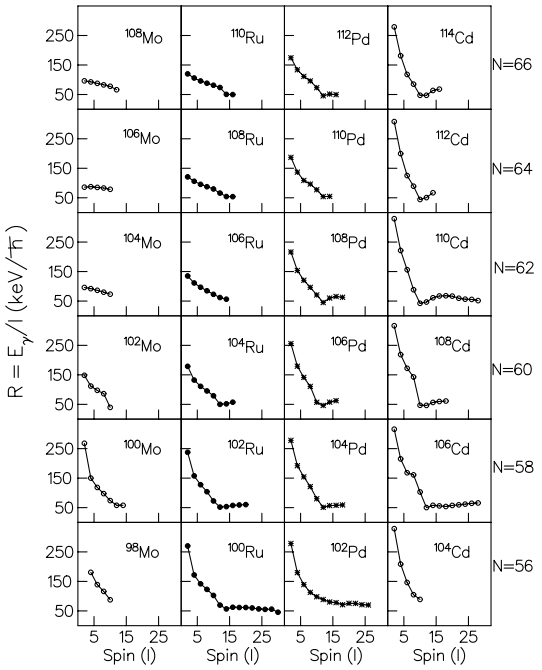

FIG. 3. E-GOS curves for the $A \sim 110$ region. These data are taken from Refs. [7,11–40].

and cadmium isotopes with $N = 60$ and 62 demonstrate this trend dramatically, with the vibrational-rotational structure change occurring around spin $10 \rightarrow 12\hbar$.

Once this weakly deformed shape is stabilized by the occupation of equatorial, high-j intruder, $h_{11/2}$ neutron orbitals, rotational motion becomes energetically favored over the lower-lying vibrational excitations. While the predicted rms quadrupole deformation values for the vibrational and rotational phases are predicted to be similar by Total Routhian Surface calculations [41] ($\langle\beta^2\rangle^{1/2} \approx 0.15$), it is the occupation of these orbitals which leads to a significant nonzero value for the static ($\gamma \approx 0°$) quadrupole deformation, β_2. A similar behavior can also be found in other regions, such as the light rare-earth nuclei with $A \sim 130$, where the low-Ω $h_{11/2}$ protons appear to play an analogous role.

Most, if not all, nominally vibrational nuclei actually exhibit a significant anharmonicity, as evidenced by the typical ratio for the excitation energies of the yrast 4^+ and 2^+ states lying closer to $2.2 \rightarrow 2.3$ rather than the harmonic limit of 2.0 [42]. In these cases, the first order expression for the level energies of an *anharmonic* vibrator given by $E_n(n = 2I) = nE_2 + \{[n(n-1)]/2\}\epsilon_4 + \ldots$, where $\epsilon_4 = E_4 - 2E_2$ and E_2 and E_4 are the excitation energies of the yrast 2^+ and 4^+ states, respectively, has been shown to work very well [43].

With this formula

$$\frac{E_\gamma}{I} = \frac{E_2}{I} - \frac{\epsilon_4}{I} + \frac{\epsilon_4}{2} = \frac{\hbar\omega}{I} - \frac{\epsilon_4}{I} + \frac{\epsilon_4}{2} \overset{I\rightarrow\infty}{\rightarrow} \frac{\epsilon_4}{2}. \quad (3)$$

For a pure harmonic vibrator ($\epsilon_4 = 0$), Eq. (3) recovers the vibrational limit of Eq. (1), while a value of $\epsilon_4 = \frac{4}{3}E_2$

recovers the axial rotor limit. For a gamma-soft nucleus [the "O(6) limit"], $E_\gamma/I = [E(2^+)/4](1 + \frac{2}{I})$, which decreases with I, but at a slower rate than for a vibrator.

In summary, we have proposed a new empirical approach based on the connection between transition energies and spin which allows one to distinguish vibrational from rotational regimes in atomic nuclei, and indeed other mesoscopic quantal systems which exhibit competing collective vibrational and rotational modes. This work also tackles the issue of structural evolution as a function of angular momentum, complementing the traditional approach of studying such changes as a function of nucleon number. New, high-spin data on ^{102}Ru vividly demonstrate the transition from a vibrator-like nucleus at low spins to a rotor when the maximally aligned neutron $(h_{11/2})^2$ configuration becomes energetically favored. The current work also highlights the potential risk of using purely rotational-based concepts (e.g., moments of inertia, backbending, rotational alignment, etc.) in spin ranges for nuclei which are not statically deformed.

This work is supported by EPSRC (U.K.) and the U.S. Department of Energy, under Grants No. DE-FG02-91ER-40609, No. DE-FG02-88ER-40417, and No. DOE-FG02-96ER-40983. P. H. R. acknowledges financial support from Yale University via both the Flint and the Science Development Funds. Professor Bill Gelletly and Dr. Carl Wheldon are thanked for their comments on this work.

[1] G. Scharff-Goldhaber and J. J. Weneser, Phys. Rev. **98**, 212 (1955).
[2] A. Bohr and B. R. Mottelson, Mat. Fys. Medd. K. Dan. Vidensk. Selsk. **27** No. 16 (1953).
[3] R. Bengtsson, S. Frauendorf, and F.-R. May, At. Data Nucl. Data Tables **35**, 15 (1986).
[4] F. S. Stephens and R. S. Simon, Nucl. Phys. **A183**, 257 (1972).
[5] C. W. Beausang *et al.*, Nucl. Instrum. Methods Phys. Res., Sect. A **452**, 431 (2000).
[6] A. Yamamoto *et al.*, Phys. Rev. C **66**, 024302 (2002).
[7] H. Dejbakhsh and S. Bouttchenko, Phys. Rev. C **52**, 1810 (1995); I. Deloncle *et al.*, Acta Phys. Pol. B **27**, 179 (1996).
[8] P. H Regan, A. E. Stuchbery, and S. S. Anderssen, Nucl. Phys. **A591**, 533 (1995).
[9] S. Frauendorf, Rev. Mod. Phys. **73**, 463 (2001).
[10] S. Zhu *et al.*, Phys. Rev. C **64**, 041302(R) (2001).
[11] R. F. Casten and N. V. Zamfir, Phys. Rep. **264**, 81 (1996).
[12] R. F. Casten, J. Jolie, H. G. Börner, D. S. Brenner, N. Z. Zamfir, W. T. Chou, and A. Aprahamian, Phys. Lett. B **297**, 19 (1992).
[13] F. Corminboeuf, T. B. Brown, L. Genilloud, C. D. Hannant, J. Jolie, J. Kern, N. Warr, and S. W. Yates, Phys. Rev. Lett. **84**, 4060 (2000).
[14] L. E. Svensson, C. Fahlander, L. Hasselgren, A. Backlin, L. Westerberg, D. Cline, T. Czosnyka, C. Y. Wu, R. M. Diamond, and H. Kluge, Nucl. Phys. **A584**, 547 (1995).
[15] L. Genilloud, T. B. Brown, F. Corminboeuf, P. E. Garrett, C. D. Hannant, J. Jolie, N. Warr, and S. W. Yates, Nucl. Phys. **A683**, 287 (2001).
[16] N. Buforn *et al.*, Eur. Phys. J. A **7**, 347 (2000).
[17] P. H. Regan *et al.*, Nucl. Phys. **A586**, 351 (1995).
[18] I. Thorslund *et al.*, Nucl. Phys. **A564**, 285 (1993).
[19] S. Juutinen *et al.*, Nucl. Phys. **A573**, 306 (1994).
[20] K. R. Pohl, P. H. Regan, J. E. Bush, P. E. Raines, D. P. Balamuth, D. Ward, A. Galindo-Uribarri, V. P. Janzen, S. M. Mullins, and S. Pilotte, Phys. Rev. C **53**, 2682 (1996).
[21] P. H. Regan *et al.*, Phys. Rev. C **55**, 2305 (1997).
[22] M. Houry *et al.*, Eur. Phys. J. A **6**, 43 (1999).
[23] R. Krücken *et al.*, Eur. Phys. J. A **10**, 151 (2001).
[24] I. Thorslund *et al.*, Nucl. Phys. **A568**, 306 (1994); M. Piiparinen *et al.*, Nucl. Phys. **A565**, 671 (1993).
[25] I. Deloncle *et al.*, Eur. Phys. J. A **8**, 177 (2000).
[26] R. B. Firestone and V. S. Shirley, *Table of Isotopes* (Wiley, New York, 1996), 8th ed., Vols. I and II.
[27] S. D. Robinson *et al.*, J. Phys. G **28**, 1415 (2002).
[28] M. Délèze, S. Drissi, J. Jolie, J. Kern, and J. P. Vorlet, Nucl. Phys. **A554**, 1 (1993).
[29] J. Gizon *et al.*, Phys. Lett. B **410**, 95 (1997).
[30] A. O. Macchiavelli *et al.*, Phys. Rev. C **38**, 1088 (1988).
[31] D. De Frenne and E. Jacobs, Nucl. Data Sheets **72**, 1 (1994).
[32] D. De Frenne and E. Jacobs, Nucl. Data Sheets **89**, 481 (2000).
[33] J. Timár, J. Gizon, A. Gizon, D. Sohler, B. M. Nyakó, L. Zolnai, A. J. Boston, D. T. Joss, E. S. Paul, A. T. Semple, C. M. Parry, and I. Ragnarsson, Phys. Rev. C **62**, 044317 (2000).
[34] D. De Frenne and E. Jacobs, Nucl. Data Sheets **89**, 481 (2000).
[35] B. Singh, Nucl. Data Sheets **84**, 565 (1998); **86**, 503(E) (1999).
[36] B. Singh, Nucl. Data Sheets **81**, 1 (1997).
[37] D. De Frenne and E. Jacobs, Nucl. Data Sheets **83**, 535 (1998).
[38] A. Guessous *et al.*, Phys. Rev. C **53**, 1191 (1996).
[39] R. Q. Xu *et al.*, Chin. Phys. Lett. **19**, 180 (2002).
[40] D. R. Haenni, H. Dejbakhsh, R. P. Schmitt, and G. Mouchaty, Phys. Rev. C **33**, 1543 (1986).
[41] W. Nazarewicz, J. Dudek, R. Bengtsson, T. Bengtsson, and I. Ragnarsson, Nucl. Phys. **A435**, 397 (1985).
[42] D. Kusnezov, N. V. Zamfir, and R. F. Casten, Phys. Rev. Lett. **85**, 1396 (2000).
[43] N. V. Zamfir and R. F. Casten, Phys. Rev. Lett. **75**, 1280 (1995).